Optical Fiber Technology 66 (2021) 102650

Contents lists available at ScienceDirect

Optical Fiber Technology

journal homepage: www.elsevier.com/locate/yofte

High-energy pulses from all-PM ultra-long Yb-fiber laser mode-locked with quasi-synchronous pumping

Boris Nyushkov [a,b,*], Aleksey Ivanenko [a], Sergey Smirnov [a], Sergey Kobtsev [a]

[a] Novosibirsk State University, Novosibirsk 630090, Russia
[b] Novosibirsk State Technical University, Novosibirsks 630073, Russia

ARTICLE INFO

Keywords:
Fiber lasers
Laser mode locking
Synchronous pumping

ABSTRACT

We explore, for the first time, mode-locking capabilities and frontiers of a quasi-synchronous pumping technique implemented in an all-polarization-maintaining (all-PM) kilometer-long Yb-fiber laser. This technically simple approach to synchronous pumping relies on sine-wave modulation of pump power at a frequency slightly detuned from the laser cavity inter-mode frequency or its multiple. In combination with the scaled-up all-PM-fiber cavity, it has provided stable generation of linearly polarized (scalar) high-energy (up to 130 nJ) pulses with tunable nanosecond duration at the fundamental and harmonic repetition rates ranging from 0.23 to 0.69 MHz. The obtained combination of such a low repetition rate, such a high energy level, and polarization stability is unique for actively mode-locked all-fiber stimulated-emission-based master oscillators. We reveal that detuning of the pump modulation frequency is the key parameter for the pulse shaping control in such mode-locked laser, and further intracavity pulse shortening towards sub-nanosecond duration is theoretically possible with measures preventing pulses from accumulation of excessive nonlinear phase. The demonstrated approach opens up new prospects for pump-modulation-based mode locking in diode-pumped lasers with such inertial active media as rare-earth-doped fibers.

1. Introduction

The unique design flexibility of mode-locked fiber lasers and their compliance with various applications drive continued research interest in novel configurations and mode locking techniques [1]. In particular, a prominent research has been dedicated to development of reliable all-fiber configurations with versatile electronic control over pulse lasing. Endeavors to implement such control in passively mode-locked all-fiber lasers have resulted in rather sophisticated inventions, such as electrically-tunable in-line saturable absorbers [2], multivariate artificial saturable absorbers [3] and machine-learning-based selection of lasing regimes [4]. In this context, active mode locking techniques should be of particular research interest because of their inherent capability for reliable electronic control of pulse lasing, as granted by the nature of active mode locking [5].

Techniques of active mode locking in fiber lasers have been advanced over the past years mainly by extensive improvement of conventional modulator-based approaches [6,7] and by novel modulating devices [8,9]. However, practically, all modulator-based techniques are more or less associated with relatively high complexity and cost, excessive intracavity losses, reduced power handling capability, and low energy efficiency. The only known modulator-free approach to active mode locking relies on synchronous pumping. It is usually applied in Raman fiber lasers [10,11] and hybrid fiber lasers with semiconductor active medium [12,13]. However, the diode-pumped fiber lasers based on the stimulated emission (such as Yb- or Er-fiber lasers) could not directly adopt this technique due to their inertial response to pumping radiation pulses (i.e., much slower laser gain recovery as compared to semiconductor-based lasers, for example). Moreover, straight implementation of this technique might require fast and deep modulation of high-power pumping laser diodes which is technically difficult. Therefore, synchronous pumping has been implemented so far only in the Tm-doped fiber lasers with the complicated pumping sources consisting of a pulsed (or modulated) master oscillator and a separate power amplifier [14,15]. Nevertheless, recently we have revealed the possibility to simplify pump-modulation-induced pulse-shaping in the stimulated-emission fiber lasers with direct diode pumping. It relies on inducing a small mismatch between the pump modulation period and the inherent group delay of laser pulses in the cavity [16].

Herein, we study, for the first time, active-mode-locking capabilities

* Corresponding author.
E-mail address: b.nyushkov@nsu.ru (B. Nyushkov).

https://doi.org/10.1016/j.yofte.2021.102650
Received 12 May 2021; Received in revised form 1 July 2021; Accepted 24 July 2021
Available online 7 August 2021

and frontiers of the proposed method in an all-PM ultra-long modulator-free Yb-doped fiber laser. It has provided stable generation of linearly-polarized (scalar) high-energy (up to 130 nJ) nanosecond pulses with tunable (down to 95 ns) duration at the fundamental and harmonic repetition rates ranging from 0.23 to 0.69 MHz upon very simple quasi-synchronous modulation of the pump power. The obtained combination of such pulse characteristics and polarization stability is unique among ever reported actively mode-locked all-fiber stimulated-emission lasers. We show also that much shorter (sub-nanosecond) pulses are theoretically obtainable.

2. Experimental setup and principle of operation

Our experimental setup is shown in Fig. 1. The laser has the all-PM ring cavity with counter-propagation of pumping and lasing waves. It consists of 0.55-m-long PM core-pumped Yb-doped fiber (LIEKKI Yb700-6/125-PM) and the following PM elements: 980/1064-nm wavelength-division multiplexor (WDM), a 30% output coupler, a 2-nm passband spectral filter centered at ~1064 nm, and an optical isolator with the fast axis blocked. Such a configuration sustains the single polarization mode and ensures scalar character of the output pulse radiation. The cavity is extended by 0.9-km-long PM fiber (Fujikura, 980 nm band PANDA fiber, PM 98-U25D-H). Incorporation of the bandpass filter was initially intended not only for rough selection of the lasing wavelength, but also for preventive suppression of supposed parasitic contributions (such as spontaneous emission and Raman scattering) to the laser output.

Pumping system consists of two PM-fiber-coupled continuous-wave laser diodes (LD) at 980 nm whose outputs are combined by using a fiber-optic polarization beam combiner (PBC). The pump radiation was sent to the laser via a pump laser protector (PLP) with a 1% tap output. The latter was used to monitor the pump power modulation. The total pump power injected into the Yb-fiber (though the intracavity WDM) reached 1.05 W at most.

Pump power was manipulated through modulation inputs of the LD current drivers. Their modulation bandwidth is limited to ~0.7 MHz (as determined at −3 dB level). The sine-wave modulating signal was synthesized by a radiofrequency arbitrary waveform generator (RF AWG). Nanosecond pulsed lasing was expected to be possible even with such slow pump modulation system, since we relied on the pulse-shortening effect revealed in our preceding work [16].

The proposed pulse shaping is based on gain discrimination of temporal laser pulse profile. It can be induced by introducing small (≤0.1%) mismatch between the pump modulation frequency f_{mod} and the fundamental pulse repetition rate f_0 (or its m-th harmonic) determined by the inherent group delay in the laser cavity. The output pulse repetition rate anyway remains equal to the pump modulation frequency ($f_{rep} = f_{mod}$) since driven oscillations always occur at the driving force frequency. However, in the case of slightly overrated modulation frequency, the laser pulse completing round trip comes to the active fiber a little bit later than if this pulse were constantly propagating with its average velocity determined by the effective round-trip time $T_{RT} = m/f_{mod}$. Then, in the active fiber, the leading edge of the pulse experiences

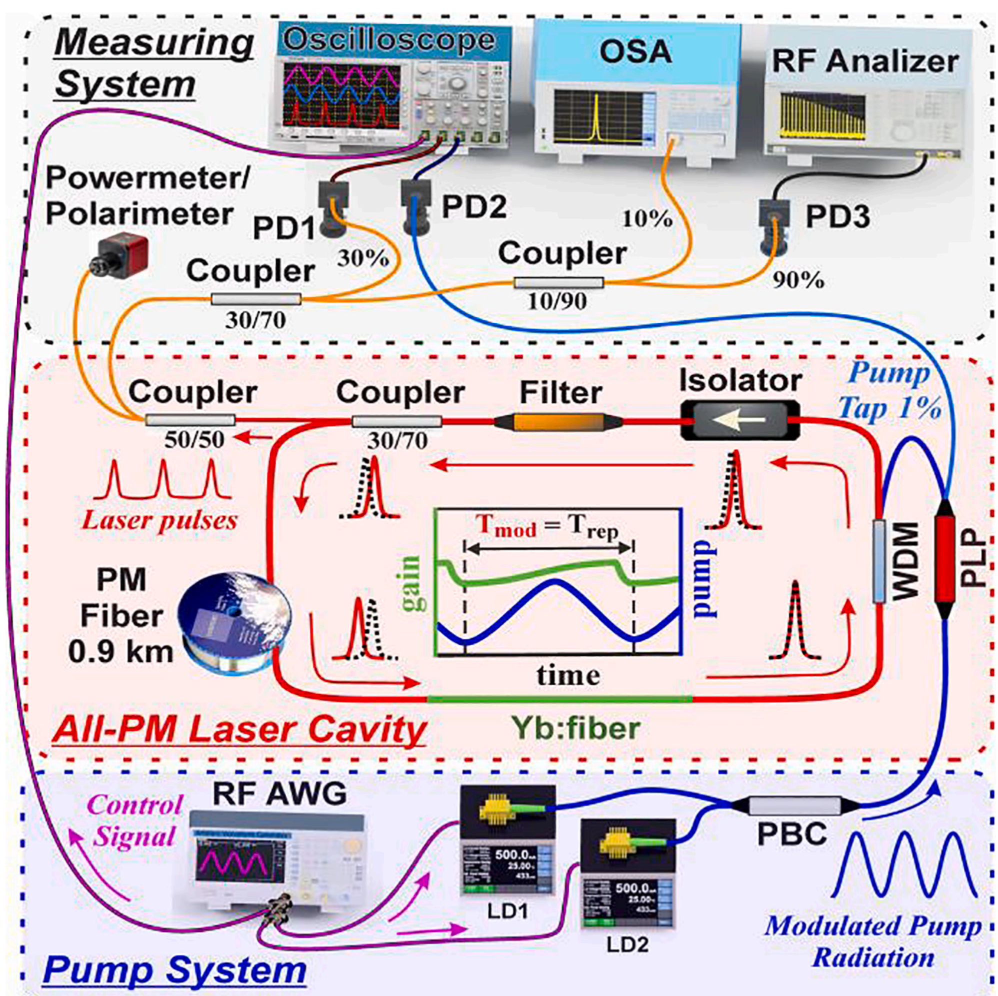

Fig. 1. Experimental setup: PD1-PD3 – photodiodes; OSA – optical spectrum analyzer; WDM – wavelength-division multiplexor; PLP – pump laser protector; PBC – polarization beam combiner; LD1, LD2 – pumping laser diodes; RF AWG – radiofrequency arbitrary waveform generator.

stronger amplification than the trailing edge (its amplification becomes lower than inverse loss) as the leading edge takes away a portion of slowly accumulated pump energy. With such pulse reshaping, the amplifier slightly "accelerates" the "retarded" pulse and thus allow stationary lasing under slightly mistimed, "quasi-synchronous", modulation.

3. Results and discussion

3.1. Experimental study

First, we have examined quasi-synchronous sine-wave pump modulation at a frequency approaching the fundamental pulse repetition rate f_0 (which is found to be 230.5 kHz).

In our experiment, the modulated pump power was always kept above the lasing threshold (90 mW) in spite of relatively high (~83%) modulation depth. The pump power was oscillating between 0.1 and 1.05 W. Fig. 2 illustrates measured evolution of spectral and time characteristics of lasing governed by tuning the modulation frequency in the vicinity of the fundamental pulse repetition rate. Downward approaching to this rate leads to gradual evolution of weakly and slowly ($T_{mod} \approx 4.35$ μs) modulated continuous-wave (CW) laser radiation into a regular train of narrow (nanosecond) pulses as confirmed by measured time traces in Fig. 2 (b, e, f). With downward frequency tuning, the pulses gradually shortened, thereby raising their peak power at constant average output power of ~37 mW. Their optical spectrum broadened simultaneously, as shown in Fig. 2(a). They finally ended up with the duration of ~205 ns (which is 21 times shorter than the modulation period) when the modulation frequency was lowered to F_L = 230.69 kHz. Further frequency lowering led to breaking of single-pulse lasing, due to the excessive nonlinear phase incursion caused by peak power rise. Thus, lasing turned to multi-pulse patterns [Fig. 2 (g)] when the modulation frequency was lowered to be between 230.69 kHz and 230.5 kHz. Below 230.5 kHz, the laser switches to weakly and slowly modulated CW lasing [Fig. 2 (h)], since the above pulse shaping is possible only with the positively detuned modulation frequencies.

The upward frequency tuning from below 230.5 kHz revealed hysteresis in the backward evolution of lasing. It returned to single-pulse operation at a higher frequency F_L^* = 230.84 kHz with a longer pulse duration of 350 ns. Thus, the downward frequency tuning is preferable, since it enables shorter single-pulse duration.

Fig. 3 demonstrates measured characteristics of a regular train of 205 ns laser pulses obtained with the downward tuning of modulation frequency to the nearly fundamental pulse repetition rate (to 230.69 kHz). Oscillograms of this pulse train testify to its high contrast (~99%) and amplitude stability (peak power fluctuations < 2%). The

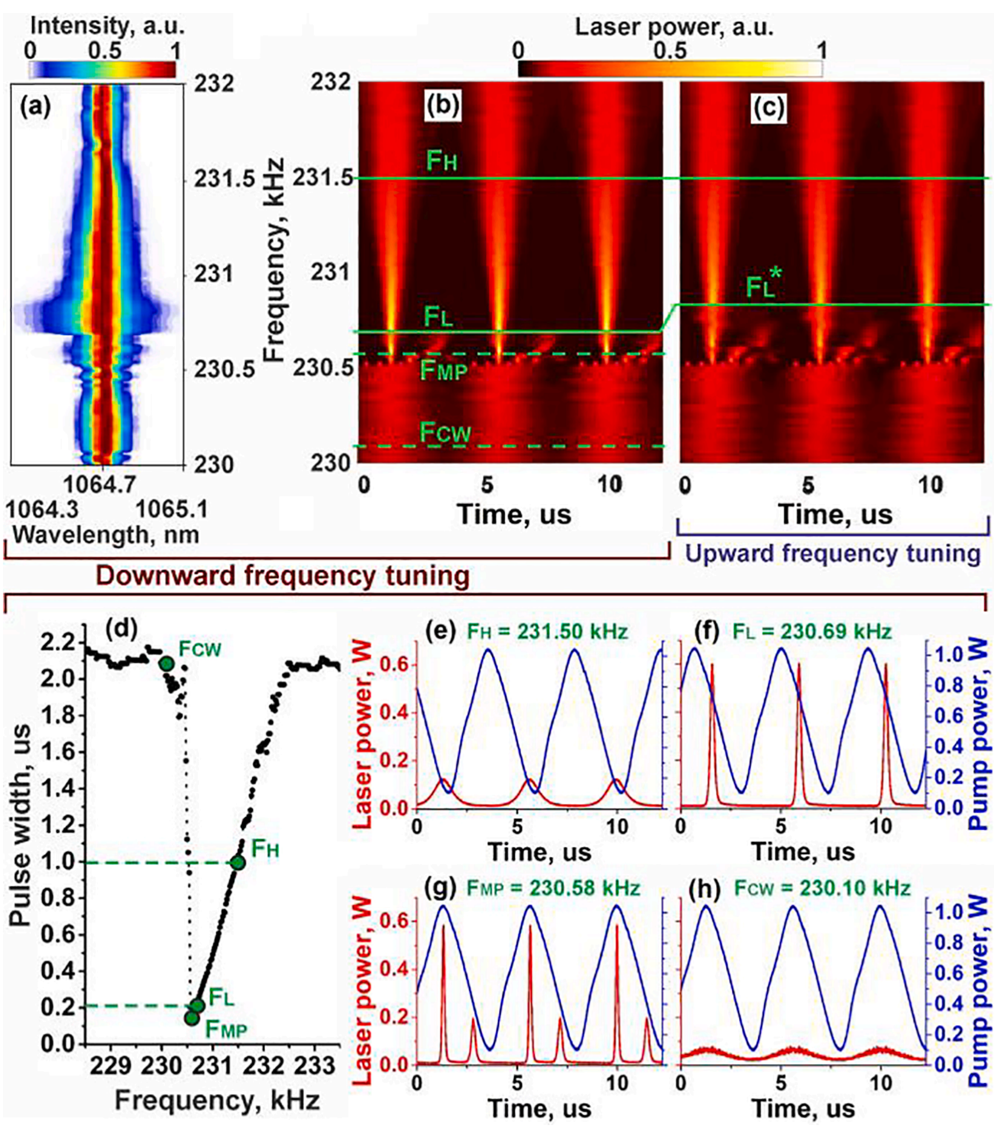

Fig. 2. Measured evolution of lasing governed by tuning the modulation frequency near the fundamental pulse repetition rate; (a–c) – spectral and temporal distributions of the laser power with respect to the frequency tuning; (d) – pulse width at half maximum versus modulation frequency; (e–h) – oscillograms of modulated pump power [blue traces] and resulting laser pulses [red traces] at the selected modulation frequencies. (For interpretation of the references to colour in this figure legend, the reader is referred to the web version of this article.)

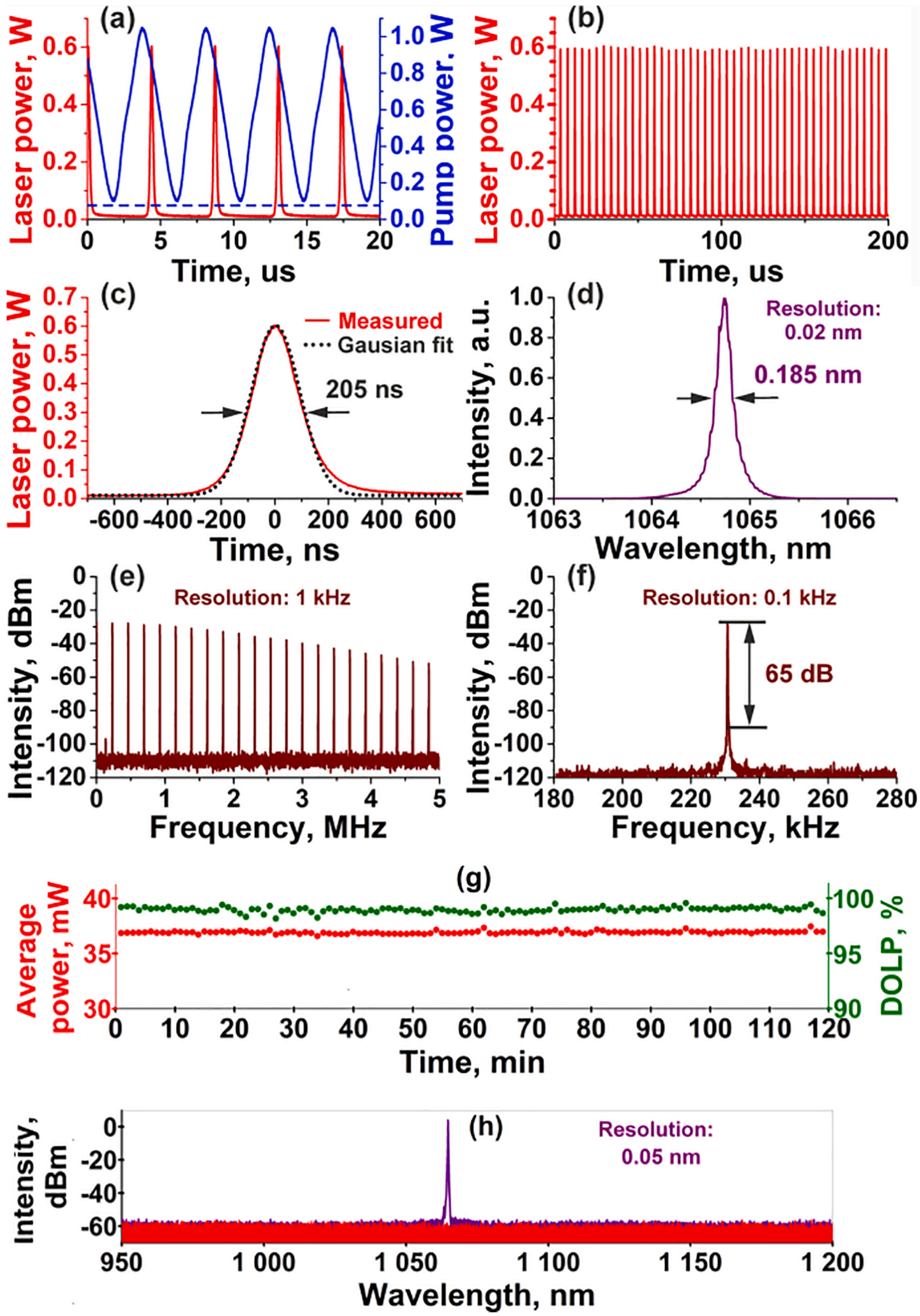

Fig. 3. Pulsed lasing at the effectively fundamental pulse repetition rate [at 230.69 kHz]; (a, b, c) – oscillograms of modulated pump power [blue trace] and resulting laser pulses [red traces]; (d) – optical spectra of laser pulses; (e, f) – radiofrequency spectra of laser pulse train; (g) – average laser power [red trace] and degree of linear polarization [DOLP, green trace] versus time; (h) – wide-range spectral scan of laser output for verification of its spectral purity (noise floor is indicated by the red line). (For interpretation of the references to colour in this figure legend, the reader is referred to the web version of this article.)

radiofrequency (RF) spectra manifest high signal-to-noise ratio (~65 dB at the actual pulse repetition frequency), and monotonic decrease of discrete spectral intensities with frequency (being consistent with Gaussian-like pulse profile). The laser pulses feature sufficient degree of integrity: relative amplitude of the coherence spike in their nonlinear autocorrelation trace was only 15%. The net pulse energy was 130 nJ at the given pulse contrast.

The obtained pulse train also features high stability in terms of polarization and average power as indicated in Fig. 3 (g). According to long-term polarimetry (performed during 2 h), the mean degree of linear polarization was as high as ~99% (standard deviation: 0.2%), the mean ellipticity was as small as 2.5° (standard deviation: 0.7°), while the standard deviation of the average power was only 0.14 mW at the mean value of 36.97 mW. Long-term stability of the pulse repetition rate was determined by the stability of the used RF AWG.

The performed wide-range spectral scan of the laser output [Fig. 3 (h)] testifies to its spectral purity and lack of noticeable contribution from Raman scattering and spontaneous emission.

Feasibility of harmonic mode locking was also examined. Fig. 4 presents characteristics of such lasing regimes obtained with the downward tuning of modulation frequency to the nearly second and nearly third harmonics of the fundamental pulse repetition rate (to 461.12 kHz and 691.61 kHz, respectively). Oscillograms of laser pulse trains obtained at harmonic repetition rates testify to the good contrast

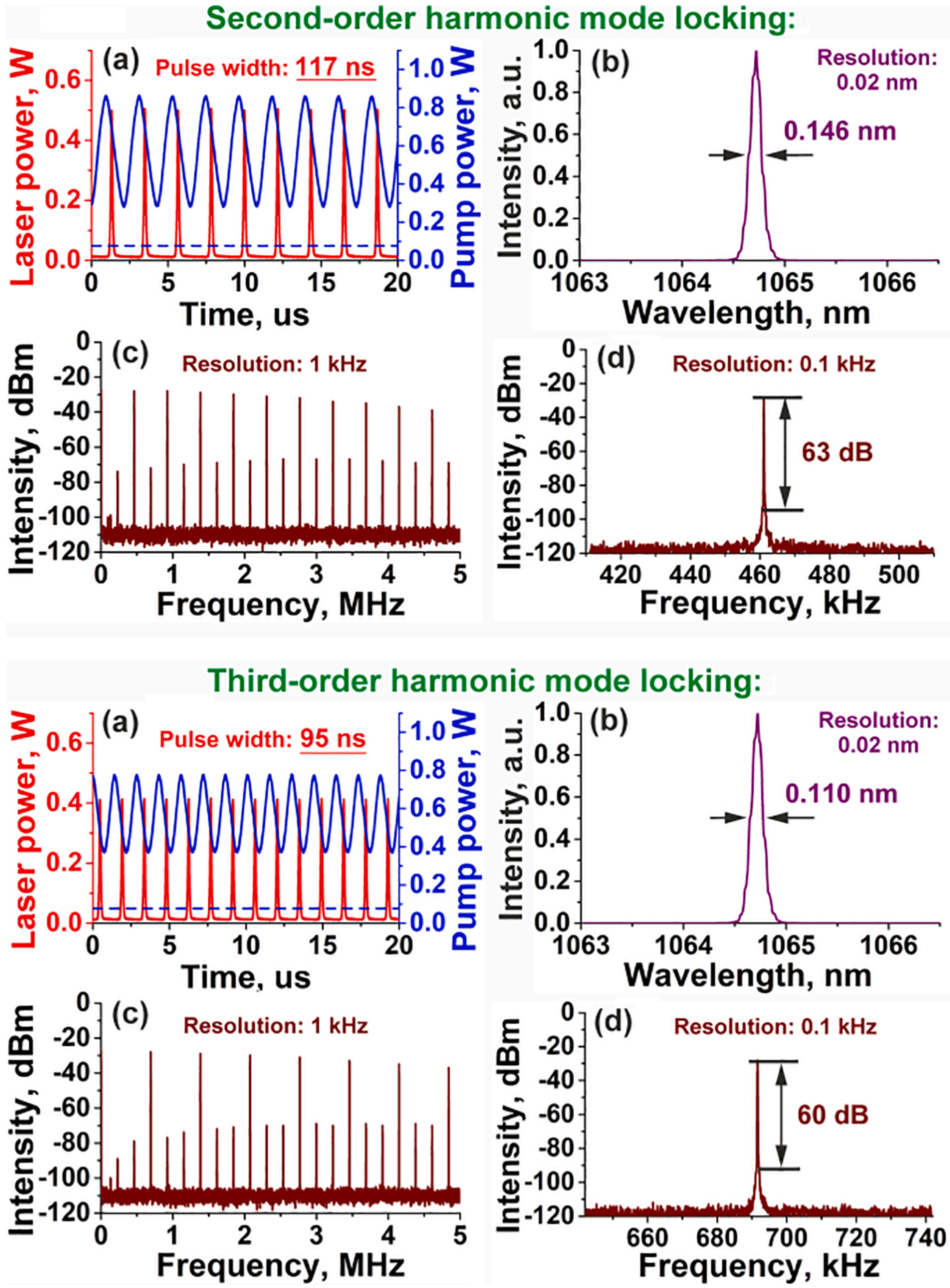

Fig. 4. Pulsed lasing at the effectively second and third harmonics of the fundamental pulse repetition rate [at 461.12 kHz and 691.61 kHz respectively]; (a) – oscillograms of modulated pump power [blue traces] and resulting laser pulse train [red traces]; (b) – optical spectra of laser pulse train; (c, d) – radiofrequency spectra of laser pulse train. (For interpretation of the references to colour in this figure legend, the reader is referred to the web version of this article.)

(nearly 98%) and acceptable amplitude stability (peak power fluctuations $< 5\%$) of those pulses. The average laser power was unaffected by switching to the harmonic mode locking and thus multiplication of pulse repetition rate led to nearly proportional reduction in the net pulse energy. It reduced to 62 nJ and 41 nJ at the 2nd and 3rd harmonics, respectively. This could also lead to the proportional reduction in peak power unless it was partially compensated by stronger pulse shortening. The pulse width (at half maximum) decreased to 117 ns and 95 ns at the 2nd and 3rd harmonics, respectively. These durations were 18.6 and 15.2 times shorter than the respective modulation periods. The decrease of the pulse shortening factor upon switching to the higher harmonics is mainly due to the parasitic reduction of the pump modulation depth. This reduction was caused by approaching to the cut-off frequency of a modulation transfer function in our pumping system. Nevertheless, the measured time traces and RF spectra validate proper quality of the obtained harmonic regimes. The RF spectra features good signal-to-noise ratio ($\sim$60 dB at the actual pulse repetition frequency) and relatively strong suppression of supermode noise. The supermode suppression ratio amounts to $\sim$40 dB (around the actual pulse repetition frequency) which is comparable with other types of harmonically mode-locked fiber lasers [17]. Obviously, use of faster LD current drivers will allow exploring of much higher orders of harmonic mode locking and consequently obtaining of much shorter pulses.

It is worth noting also that the obtained pulsed radiation is relatively narrowband in comparison with the much wider pass band of the intracavity filter. This ensures that the studied time-domain gain-governed pulse shaping is not noticeably affected by spectral filtering. The laser pulses feature relatively narrow optical spectrum due to moderate nonlinear phase incursion which is considered in the following section.

3.2. Theoretical analysis

To determine inherent theoretical limits of the above pulse shaping mechanism in terms of pulse shortening, we studied it also numerically. To that end, a transport equation with gain and loss terms describing lasing with neglectable optical nonlinearity and dispersion was solved in order to consider the gain-governed pulse shaping:

$$\frac{n}{c}\frac{\partial P_s}{\partial t}+\frac{\partial P_s}{\partial z}+\alpha P_s+\alpha_c P_s\delta(z-z_c)-gP_s\delta(z-z_a)=0, \tag{1}$$

where t and z denote time and space coordinates along the fiber, P_s is intracavity signal power, c is the velocity of light in vacuum, $n = 1.45$ is effective refractive index of optical fiber, $\alpha = 1.47\ \mathrm{km}^{-1}$ denotes effective (distributed) intracavity optical losses, while $\alpha_c = 0.70$ stands for lumped losses at the 30% output coupler (its coordinate is z_c), g is optical amplification coefficient. Amplification was assumed to be lumped, since the active fiber is much shorter than total cavity length: $g(z)\propto\delta(z-z_a)$; z_a is the coordinate of the optical amplifier.

The procedure of numerical integration of Eq. (1) was similar to that described in [16] numerically: we used a uniform mesh with $N = 2^{11} = 2\,048$ points and step size $h \sim 0.49$ m for integration over space, and a temporal mesh with the step $hn/c \sim 2.4$ ns for integration over time. The results were reproduced on meshes with different number of points ranging from 2^{11} up to 2^{13} for validation.

Optical amplification in the Yb-doped fiber was simulated by solving numerically Eq. (5) from Ref. [18] which allows modeling such an active fiber as an effectively two-level laser medium. For the simulation, we used the following values of the active fiber cross-section (provided by the fiber supplier): $\sigma^{(p)}{}_{12} = 1.51 \times 10^{-20}\ \mathrm{cm}^2$, $\sigma^{(p)}{}_{21} = 1.80 \times 10^{-20}\ \mathrm{cm}^2$, $\sigma^{(s)}{}_{12} = 4.48 \times 10^{-23}\ \mathrm{cm}^2$, $\sigma^{(s)}{}_{21} = 2.36 \times 10^{-21}\ \mathrm{cm}^2$, as well as the following values of normalized pump and signal power distributions at the fiber core center: $\rho_p(0) = \rho_s(0) = 3.6 \times 10^6\ \mathrm{cm}^{-2}$.

The calculated evolution of pulse lasing governed by tuning the modulation frequency is shown in Fig. 5. It is in a very good agreement with the measured evolution over the major part of the frequency tuning range, except the immediate vicinity of the fundamental pulse repetition rate f_0 (at a residual relative detuning $\delta f/f_0 < 10^{-3}$). In this vicinity, the experimental narrowing of laser pulse finished up with pulse breaking and switching to multi-pulse lasing, while the theoretical evolution turned to be nearly pulse-breaking-free. It predicts further pulse narrowing upon closer approach to the fundamental repetition rate provided that the frequency tuning step is small enough (0.3 Hz herein), optical nonlinearity and dispersion are negligible. Thus, theoretically it might be possible to make pulse as short as $\sim 10^{-3}$ of the modulation period as suggested by Fig. 5 (d).

However, in practice, laser pulse shortening leads to a corresponding rise in the laser peak power and consequently causes an adequate in-

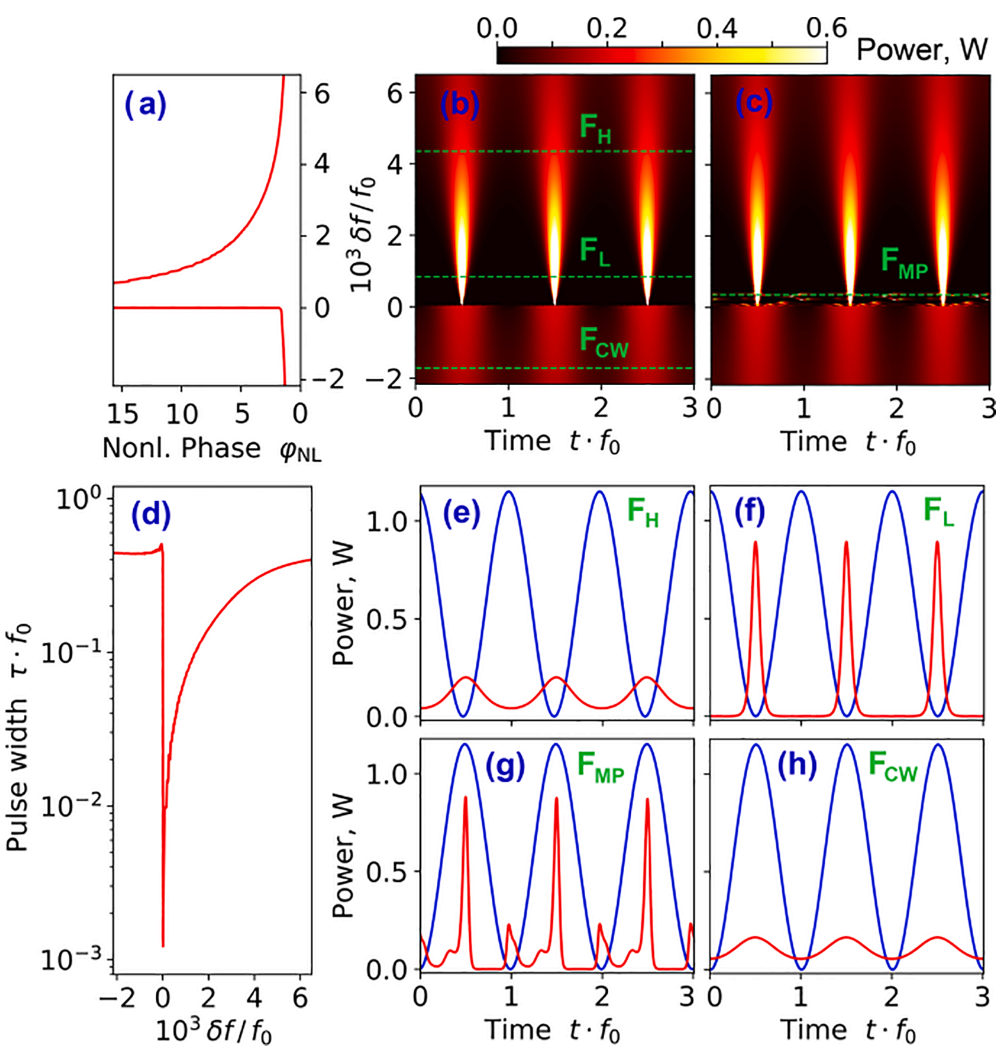

Fig. 5. Calculated evolution of pulse lasing governed by tuning the modulation frequency near the fundamental pulse repetition rate; (a) – accumulated nonlinear phase [in radians] versus relative detuning of the modulation frequency [δf / f_0]; (b, c) – temporal distributions of the laser power with respect to the downward and upward frequency tuning; (d) – pulse width versus relative frequency detuning; (e–h) – time traces of pump power oscillations [blue] and resulting laser pulses [red] at the selected frequency tuning stages. (For interpretation of the references to colour in this figure legend, the reader is referred to the web version of this article.)

crease of the nonlinear phase φ_{NL} which is accumulated by the laser pulse upon propagation through the ultra-long fiber cavity:

$$\varphi_{NL} = \int_0^L \gamma P_s(z)dz, \tag{2}$$

where L denotes the fiber cavity length, γ is the nonlinear coefficient of the fiber used to produce the cavity. Fig. 5 (a) shows calculated evolution of the nonlinear phase which would accompany continuous pulse shortening governed by downward frequency tuning. In the experiment, the minimal frequency detuning (which allows single-pulse lasing with the shortest pulse duration) was about 0.82×10^{-3}. According to calculations, such short pulses have to accumulate the nonlinear phase of about 4π. Further pulse shortening would lead to much higher values. In principle, all-normal-dispersion (ANDi) mode-locked fiber lasers can tolerate accumulation of higher nonlinear phase [19]. However, our laser configuration does not fall into the conventional concept of ANDi mode-locked lasers due to the lack of intracavity saturable absorber or intensity modulator. Nevertheless, we believe that the introduced laser configuration can be further optimized by management of the intracavity peak power, similarly to the power management proposed earlier in [20]. The primary approach relies on adjustment of the output coupling ratio in order to reduce residual radiation power at the input of the ultra-long intracavity fiber span. It will reduce accumulation of the nonlinear phase and consequently allow stronger pulse shortening as suggested by the theoretical model.

It is worth noting that there is also another kind of limit to power (and energy) scaling in long fiber lasers. This limit is imposed by Raman scattering [21,22]. Therefore, it is important to consider also such a possible frontier of the studied mode-locked operation. Taking into account relatively long duration of the generated laser pulses, we used a classical formula (derived differently by R.G. Smith [23] and by L. de la Cruz-May et al [24]) for estimation of the critical power P_0^{Cr} for stimulated Raman scattering (SRS) in the ultra-long passive fiber span used in our laser:

$$P_0^{Cr} \approx 16\frac{A_{eff}}{g_R L_{eff}}, \tag{3}$$

where A_{eff} is the effective mode area of the fiber, g_R is the Raman gain coefficient, and L_{eff} is the effective fiber length. According to Eq. (3), the critical power for the used ultra-long intracavity fiber span is about 8 W, which is much higher than the actual intracavity peak power (about 1.4 W at the input of ultra-long passive fiber span, as determined from the measurements). Thus, the actual laser performance is quite far from the critical power. Possible approaching to this power upon further pulse shortening (and corresponding rise in the laser peak power) may become an issue, but it can be avoided with the help of the above mentioned intracavity peak power management.

4. Conclusion

To summarize, we have explored capabilities of a very simple and efficient modulator-free approach to active mode locking in all-PM ultra-long Yb-fiber lasers. Quasi-synchronous pump modulation, along with polarization-maintaining cavity elongation, has allowed stable generation of linearly-polarized (scalar) high-energy (up to 130 nJ) pulses with adjustable nanosecond duration at sub-MHz repetition rates. Such characteristics in combination with the long-term polarization stability make the laser unique among ever reported actively mode-locked all-fiber stimulated-emission lasers. Despite significant progress in the development of ultra-long fiber lasers with passive mode locking [20,25,26], the proposed active mode-locking method can be a profitable alternative in many cases due to a very simple, reliable and cheap laser design that does not employ any saturable absorbers or optical modulators. Due to these features, such a high-quality master oscillator being assisted by an amplifier may find application in lidar measurements (remote sensing) [27], material micro-processing [28] or other tasks in which high-energy pulsed radiation with stable strictly-determined parameters (along with tunability of pulse duration and peak power) is required. It is also worth noting that the spectral bandwidth of the demonstrated pulse lasing is rather small (of the order of 0.1 nm) which may be advantageous to some other applications of stable nanosecond laser sources [29].

Moreover, the developed approach breaks restrictions and obstacles which are supposed to be on the way to synchronous pumping in diode-pumped lasers with such inertial active media as rare-earth-doped fibers. The method greatly relaxes requirements to modulation speed of pumping diodes, and provides nanosecond pulse shaping regardless of the millisecond lifetime of the upper laser level. We have also considered possibility of further intracavity pulse shortening towards sub-nanosecond duration, relying on higher-order harmonic mode locking and peak power management.

CRediT authorship contribution statement

Boris Nyushkov: Conceptualization, Investigation, Formal analysis, Writing - original draft. **Aleksey Ivanenko:** Software, Investigation, Visualization. **Sergey Smirnov:** Software, Formal analysis, Writing - review & editing. **Sergey Kobtsev:** Project administration, Funding acquisition, Writing - review & editing.

Declaration of Competing Interest

The authors declare that they have no known competing financial interests or personal relationships that could have appeared to influence the work reported in this paper.

Acknowledgments

This research was supported by Russian Science Foundation under Grant 17-12-01281. The used simulation software was developed with support from Ministry of Science and Higher Education of the Russian Federation in the frame of the task FSUS-2020-0036. The developed laser was tested for material microprocessing capability at NSTU Materials Research Center.

References

[1] Y. Han, Y. Guo, B. Gao, C. Ma, R. Zhang, H. Zhang, Generation, optimization, and application of ultrashort femtosecond pulse in mode-locked fiber lasers, Prog. Quantum. Electron. 71 (2020), 100264.
[2] E.J. Lee, S.Y. Choi, H. Jeong, N.H. Park, W. Yim, M.H. Kim, J.-K. Park, S. Son, S. Bae, S.J. Kim, K. Lee, Y.H. Ahn, K.J. Ahn, B.H. Hong, J.-Y. Park, F. Rotermund, D.-I. Yeom, Active control of all-fibre graphene devices with electrical gating, Nat. Commun. 6 (2015) 6851.
[3] A. Kokhanovskiy, S. Kobtsev, A. Ivanenko, S. Smirnov, Properties of artificial saturable absorbers based on NALM with two pumped active fibres, Laser Phys. Lett. 15 (12) (2018), 125101.
[4] G. Genty, L. Salmela, J.M. Dudley, D. Brunner, A. Kokhanovskiy, S. Kobtsev, S. K. Turitsyn, Machine learning and applications in ultrafast photonics, Nat. Photon. 15 (2) (2021) 91–101.
[5] A.M. Perego, B. Garbin, F. Gustave, S. Barland, F. Prati, G.J. Valcárcel, Coherent master equation for laser modelocking, Nat. Commun. 11 (2020) 311.
[6] H. Chen, S.-P. Chen, Z.-F. Jiang, J. Hou, Versatile long cavity widely tunable pulsed Yb-doped fiber laser with up to 27655th harmonic mode locking order, Opt. Express 23 (2) (2015) 1308–1318.
[7] R. Wang, Y. Dai, F. Yin, X.u. Kun, L.i. Yan, J. Li, J. Lin, High-repetition-rate, stretch-lens-based actively-mode-locked femtosecond fiber laser, Opt. Express 21 (18) (2013) 20923–20930.
[8] J. Kim, J. Koo, J.H. Lee, All-fiber acousto-optic modulator based on a cladding-etched optical fiber for active mode-locking, Photon. Res. 5 (5) (2017) 391–395.
[9] B. Nyushkov, A. Ivanenko, S. Smirnov, O. Shtyrina, S. Kobtsev, Triggering of different pulsed regimes in fiber cavity laser by a waveguide electro-optic switch, Opt. Express 28 (10) (2020) 14922–14932.
[10] S. Kobtsev, S. Kukarin, A. Kokhanovskiy, Synchronously pumped picosecond all-fibre Raman laser based on phosphorus-doped silica fibre, Opt. Express 23 (14) (2015) 18548–18553.

[11] D.S. Kharenko, V.D. Efremov, E.A. Evmenova, S.A. Babin, Generation of Raman dissipative solitons near 1.3 microns in a phosphosilicate-fiber cavity, Opt. Express 26 (12) (2018) 15084–15089.

[12] N.V. Pedersen, K.B. Jakobsen, M. Vaa, Mode-locked 1.5 μm semiconductor optical amplifier fiber ring, J. Lightwave Technol. 14 (5) (1996) 833–838.

[13] B. Nyushkov, A. Ivanenko, S. Smirnov, S. Kobtsev, Electronically controlled generation of laser pulse patterns in a synchronously pumped mode-locked semiconductor optical amplifier-fiber laser, Laser Phys. Lett. 16 (11) (2019), 115103.

[14] G. Li, Y. Zhou, S.-J. Li, P. Yao, W. Gao, C. Gu, L.-X. Xu, Synchronously pumped mode-locked 1.89μm Tm-doped fiber laser with high detuning toleration, Chin. Phys. Lett. 35 (11) (2018), 114203.

[15] Y. Wang, S.Y. Set, S. Yamashita, Active mode-locking via pump modulation in a Tm-doped fiber laser, APL Photon. 1 (2016), 071303.

[16] S.V. Smirnov, B.N. Nyushkov, A.V. Ivanenko, D.B. Kolker, S.M. Kobtsev, Shaping of nanosecond pulses in ytterbium fiber lasers by synchronous sine-wave pump modulation, J. Opt. Soc. Am. B 37 (10) (2020) 3068–3076.

[17] C. Mou, R. Arif, A. Rozhin, S. Turitsyn, Passively harmonic mode locked erbium doped fiber soliton laser with carbon nanotubes based saturable absorber, Opt. Mater. Express 2 (6) (2012) 884–890.

[18] S.K. Turitsyn, A.E. Bednyakova, M.P. Fedoruk, A.I. Latkin, A.A. Fotiadi, A. S. Kurkov, E. Sholokhov, Modeling of CW Yb-doped fiber lasers with highly nonlinear cavity dynamics, Opt. Express 19 (9) (2011) 8394–8405.

[19] F.W. Wise, A. Chong, W.H. Renninger, High-energy femtosecond fiber lasers based on pulse propagation at normal dispersion, Laser Photon. Rev. 2 (1-2) (2008) 58–73.

[20] A. Ivanenko, S. Kobtsev, S. Smirnov, A. Kemmer, Mode-locked long fibre master oscillator with intra-cavity power management and pulse energy $>$ 12 μJ, Opt. Express 24 (6) (2016) 6650–6655.

[21] D.S. Kharenko, E.V. Podivilov, A.A. Apolonski, S.A. Babin, 20 nJ 200 fs all-fiber highly chirped dissipative soliton oscillator, Opt. Lett. 37 (19) (2012) 4104–4106.

[22] C. Aguergaray, A. Runge, M. Erkintalo, N.G.R. Broderick, Raman-driven destabilization of mode-locked long cavity fiber lasers: fundamental limitations to energy scalability, Opt. Lett. 38 (15) (2013) 2644–2646.

[23] R.G. Smith, Optical power handling capacity of low loss optical fibers as determined by stimulated Raman and Brillouin scattering, Appl. Opt. 11 (11) (1972) 2489–2494.

[24] L. de la Cruz-May, J.A. Álvarez-Chavez, E.B. Mejía, A. Flores-Gil, F. Mendez-Martinez, S. Wabnitz, Raman threshold for nth-order cascade Raman amplification, Opt. Fiber Technol. 17 (3) (2011) 214–217.

[25] R.I. Woodward, E.J.R. Kelleher, T.H. Runcorn, S. Loranger, D. Popa, V.J. Wittwer, A.C. Ferrari, S.V. Popov, R. Kashyap, J.R. Taylor, Fiber grating compression of giant-chirped nanosecond pulses from an ultra-long nanotube mode-locked fiber laser, Opt. Lett. 40 (3) (2015) 387–390.

[26] F. Gallazzi, M. Jimenez-Rodriguez, E. Monroy, P. Corredera, M. González-Herráez, F.B. Naranjo, J.D. Ania Castañón, Sub-250 fs passively mode-locked ultralong ring fibre oscillators, Opt. Laser Technol. 138 (2021), 106848.

[27] F. Di Teodoro, P. Belden, P. Ionov, N. Werner, High-power ns-pulse fiber laser sources for remote sensors, Opt. Fiber Technol. 20 (6) (2014) 688–693.

[28] W.P. Davis, S.T. Hendow, R. Kovacevic, Sinusoidal surface texturing using a nanosecond pulsed MOPA fiber laser, in: Proc. International Congress on Applications of Lasers & Electro-Optics, Orlando, Florida, USA, 2011, pp. 1131–1136.

[29] M. Kues, C. Reimer, B. Wetzel, P. Roztocki, B.E. Little, S.T. Chu, T. Hansson, E. A. Viktorov, D.J. Moss, R. Morandotti, Passively mode-locked laser with an ultra-narrow spectral width, Nat. Photon. 11 (3) (2017) 159–162.